Transcriptional integration of the responses to iron availability in Arabidopsis by the bHLH factor ILR3

Nicolas Tissot, Kevin Robe, Fei Gao, Susana Grant-Grant, Jossia Boucherez, Fanny Bellegarde, Amel Maghiaoui, Romain Marcelin, Esther Izquierdo, Moussa Benhamed, et al.

New Phytologist

Research

Transcriptional integration of the responses to iron availability in Arabidopsis by the bHLH factor ILR3

Nicolas Tissot[1], Kevin Robe[1]*, Fei Gao[1]*, Susana Grant-Grant[3], Jossia Boucherez[1], Fanny Bellegarde[1], Amel Maghiaoui[1], Romain Marcelin[1], Esther Izquierdo[1], Moussa Benhamed[2], Antoine Martin[1], Florence Vignols[1], Hannetz Roschzttardtz[3], Frédéric Gaymard[1], Jean-François Briat[1] and Christian Dubos[1]

[1]BPMP, Univ Montpellier, CNRS, INRA, SupAgro, 34060 Montpellier, France; [2]Institut of Plant Sciences Paris-Saclay (IPS2), UMR 9213/UMR1403, CNRS, INRA, Université Paris-Sud, Université d'Evry, Université Paris-Diderot, Sorbonne Paris-Cité, Bâtiment 630, 91405 Orsay, France; [3]Departamento de Genética Molecular y Microbiología, Pontificia Universidad Católica de Chile, 8331150 Santiago, Chile

Author for correspondence:
Christian Dubos
Tel: +33 4 99 61 28 18
Email: Christian.dubos@inra.fr

Received: *8 November 2018*
Accepted: *12 February 2019*

New Phytologist (2019) **223:** 1433–1446
doi: 10.1111/nph.15753

Key words: *Arabidopsis thaliana*, basic helix–loop–helix, bHLH105, ferritins, homeostasis, ILR3, iron, PYE.

Summary

- Iron (Fe) homeostasis is crucial for all living organisms. In mammals, an integrated posttranscriptional mechanism couples the regulation of both Fe deficiency and Fe excess responses. Whether in plants an integrated control mechanism involving common players regulates responses both to deficiency and to excess is still to be determined.
- In this study, molecular, genetic and biochemical approaches were used to investigate transcriptional responses to both Fe deficiency and excess.
- A transcriptional activator of responses to Fe shortage in Arabidopsis, called bHLH105/ILR3, was found to also negatively regulate the expression of ferritin genes, which are markers of the plant's response to Fe excess. Further investigations revealed that ILR3 repressed the expression of several structural genes that function in the control of Fe homeostasis. ILR3 interacts directly with the promoter of its target genes, and repressive activity was conferred by its dimerisation with bHLH47/PYE. Last, this study highlighted that important facets of plant growth in response to Fe deficiency or excess rely on ILR3 activity.
- Altogether, the data presented herein support that ILR3 is at the centre of the transcriptional regulatory network that controls Fe homeostasis in Arabidopsis, in which it acts as both transcriptional activator and repressor.

Introduction

The control of iron (Fe) homeostasis is essential in all living organisms. Perturbations of Fe uptake, circulation, metabolism or storage alter plant productivity and the quality of their derived products (Briat *et al.*, 2015). Although Fe is one of the most abundant elements found in soils, it is generally poorly available to plants because it is mainly present in the form of insoluble chelates. This is, for instance, found for calcareous soils that represent one-third of the world's cultivated lands (Guerinot & Yi, 1994). Therefore, decrypting the physiological and molecular mechanisms governing plant Fe uptake, transport and storage is a critical issue considering that all the Fe that is present in the human diet comes, directly or indirectly, from plants.

Plants respond to Fe shortage through different mechanisms (Kobayashi & Nishizawa, 2012). Nongraminaceous monocot as well as dicot species such as *Arabidopsis thaliana* have evolved a reduction-based strategy to solubilise and absorb Fe from the soil (Morrissey & Guerinot, 2009; Brumbarova *et al.*, 2015; Curie & Mari, 2016; Connorton *et al.*, 2017). It relies on the reduction of Fe(III) chelates present in the soil by FRO2 (FERRIC REDUCTION OXIDASE 2) (Robinson *et al.*, 1999). The Fe^{2+} ion generated is then transported across the rhizodermis cell membranes by IRT1 (IRON-REGULATED TRANSPORTER 1) (Eide *et al.*, 1996; Henriques *et al.*, 2002; Varotto *et al.*, 2002; Vert *et al.*, 2002). This process is facilitated by the activity of the AHA2 proton-ATPase, whose activity leads to rhizosphere acidification (Santi & Schmidt, 2009). In addition, Fe solubilisation is enhanced by the excretion (by the rhizodermis-specific PDR9/ABCG37 transporter) of Fe-mobilising phenolic compounds (Fourcroy *et al.*, 2004, 2014, 2016; Rodríguez-Celma *et al.*, 2013a; Schmid *et al.*, 2014). Fe transport, compartmentalisation and storage is also modulated in response to fluctuations in Fe availability (Morrissey & Guerinot, 2009; Kobayashi & Nishizawa, 2012; Brumbarova *et al.*, 2015; Curie & Mari, 2016; Connorton *et al.*, 2017).

Plant response to Fe deficiency is tightly regulated at the transcriptional level by a complex transcriptional regulatory cascade in which basic helix–loop–helix (bHLH) transcription factors (TFs) play a predominant role (Heim *et al.*, 2003; Gao *et al.*, 2019). In Arabidopsis, the main TFs involved have been characterised. At the top of this regulatory network, four bHLH TFs

*These authors contributed equally to this work.

(bHLH34, bHLH104, bHLH105/ILR3 – IAA-LEUCINE RESISTANT3, and bHLH115) form homo- and heterodimers that regulate the expression of five additional bHLH TFs (Zhang *et al.*, 2015; Li *et al.*, 2016; Liang *et al.*, 2017). Targeted TFs consist of *bHLH38*, *bHLH39*, *bHLH100*, *bHLH101* and *bHLH47/PYE* (*POPEYE*) (Colangelo & Guerinot, 2004; Wang *et al.*, 2007, 2013; Yuan *et al.*, 2008; Zhang *et al.*, 2015). Once induced, bHLH38, bHLH39, bHLH100, bHLH101 can form heterodimers with bHLH29/FIT (FE-DEFICIENCY INDUCED TRANSCRIPTION FACTOR) (Colangelo & Guerinot, 2004; Jakoby *et al.*, 2004; Yuan *et al.*, 2008). Then, these FIT-dependent transcriptional complexes activate the transcription of genes encoding for the Fe uptake system (for example *FRO2*, *IRT1*) located at the root epidermis (Vert *et al.*, 2002; Yuan *et al.*, 2008; Wang *et al.*, 2013). Four additional bHLH partners of FIT (bHLH18, bHLH19, bHLH20, and bHLH25) promote its degradation in response to jasmonic acid induction, antagonising the activity of bHLH38, bHLH39, bHLH100, bHLH101 and hence Fe uptake (Cui *et al.*, 2018). By contrast, PYE is a transcriptional repressor that contains in its C-terminal part an EAR motif (DLNxxP), one of the most predominant form of transcriptional repression motif identified in plants (Kagale & Rozwadowski, 2011). For instance, in the root pericycle, PYE represses the expression of genes notably implicated in Fe transport such as *NAS4* (*NICOTIANAMINE SYNTHASE 4*), a key gene involved in phloem-based transport of Fe to sink organs (Klatte *et al.*, 2009; Long *et al.*, 2010). PYE was shown to heterodimerise *in vivo* with bHLH104, ILR3 and bHLH115 (Long *et al.*, 2010; Zhang *et al.*, 2015). However, it is still unclear if these interactions play a role in the plant response to Fe deficiency or in the control of Fe homeostasis.

Under aerobic conditions, Fe can react with H_2O_2 (Fenton reaction) producing reactive oxygen species (ROS) that are deleterious to the cell. This property renders Fe excess detrimental for plant growth, severely affecting crop yield (Becker, 2005; Khabaz-Saberi, 2010). Regulation of Fe excess responses in plants has been studied at cellular and molecular levels mostly by using the *AtFER1* gene as a model. *AtFER1* encodes the most expressed Fe storage ferritin protein in Arabidopsis vegetative tissues whose expression and protein abundance is strongly induced in response to Fe excess (Petit *et al.*, 2001; Duc *et al.*, 2009; Briat *et al.*, 2010; Bournier *et al.*, 2013; Reyt *et al.*, 2015).

This is by contrast with the animal systems in which the balance between Fe uptake and storage is mainly achieved by the posttranscriptional regulation of ferritin and transferrin receptor synthesis by the iron-responsive protein element (IRE)/iron-reponsive protein (IRP1)−cytosolic aconitase Fe switch (Hentze *et al.*, 2010). Briefly, specific sequences, named IREs and found in the 5′-untranslated region (UTR) of ferritin mRNA and in the 3′-UTR of transferrin receptor transcript, function as binding sites for related *trans*-acting factors, named IRPs. In the case of Fe deficiency, IRPs are bound to IREs. Consequently, the translation of the ferritin mRNA is inhibited, avoiding Fe storage, and the transferrin receptor mRNA is stabilised, leading to an increase in abundance of the corresponding protein, which promotes Fe uptake. By contrast, Fe excess leads to IRPs dissociation from IREs, promoting ferritin mRNA translation and Fe storage on the one hand, and transferrin receptor mRNA degradation and Fe uptake inhibition on the other hand. Under Fe excess conditions, some IRPs contain a 4Fe−4S cluster, conferring to them a cytosolic aconitase activity, whereas others that do not contain such a cluster are degraded. If the Fe deficiency and Fe excess responses are controlled in plants by an integrated pathway involving common players, as it is the case in mammals (Hentze *et al.*, 2010), is therefore an important issue that remains to be addressed.

In this study, by combining molecular, genetic and biochemical approaches, ILR3 was found to act as a repressor of *AtFER1* gene expression in vegetative tissues. Expression studies together with chromatin immunoprecipitation (ChIP) assays highlighted that ILR3 represses the expression of structural genes involved in the control of Fe homeostasis through the direct binding to their promoter and that ILR3 repressive activity is conferred by its dimerisation with PYE. The use of *ilr3* mutants (loss-of-function and dominant mutations), as well as a triple ferritin mutant, indicated that several facets of plant growth in response to fluctuations in Fe availability, from deficiency to excess, rely on ILR3 and ferritin activities. Altogether, the data presented here indicate that ILR3 function extends beyond the sole control of bHLH TFs expression upstream of the Fe deficiency transcriptional regulatory network and therefore support the theory that ILR3 plays a critical role in the transcriptional regulatory network that controls Fe homeostasis in Arabidopsis, where it acts as both transcriptional activator and repressor.

Materials and Methods

Arabidopsis gene IDs

APX1, At1g07890; *AtFER1*, At5g01600; *AtFER3*, At3g56090; *AtFER4*, At2g40300; *At-NEET*, At5g51720; *bHLH34*, At3g23210; *bHLH39*, At3g56980; *bHLH47/PYE*, At3g47640; *bHLH104*, At4g14410; *bHLH105/ILR3*, At5g54680; *bHLH115*, At1g51070; *IRT1*, At4g19690; *PP2AA3*, At1g13320; *NAS4*, At1g56430; *VTL2*, At1g76800.

Plant materials

Arabidopsis thaliana ecotype Columbia (Col-0) was used as the wild-type (WT). The following mutant lines were used in this study: *bhlh34* (Li *et al.*, 2016), *bhlh104-1* (Zhang *et al.*, 2015), *ilr3-1* (Rampey *et al.*, 2006), *ilr3-3* (Li *et al.*, 2016), *pye-1* (Long *et al.*, 2010), *ilr3-3 pye-1* (this study), *bhlh115-2* (Liang *et al.*, 2017) and *fer1,3,4* (Ravet *et al.*, 2009).

Growth conditions

In vitro cultures: Seedlings were grown under long day conditions (16 h : 8 h, light : dark) on half strength Murashige and Skoog medium (½MS) with 0.05% MES, 1% sucrose, 0.7% agar for 7–10 d. Fe concentration was 50 μM and provided as Fe(III)-EDTA. For GUS experiments as well as for qRT-PCR, western and ChIP analyses, seedlings were transferred from agar plates to

liquid ½MS medium for an additional 3 days of growth in the absence or presence of Fe (50 μM Fe(III)-citrate), corresponding to the Fe deficiency (−Fe) or control (C) conditions, respectively. Fe excess (+Fe) treatment was applied by adding 500 μM Fe-citrate for 6 h to the growth solution for plants grown in the absence of Fe. For root length and fresh weight measurements, seedlings were grown on solid ½MS for 2 wk in the presence or absence of Fe(III)-EDTA (C, −Fe and +Fe). Root length was measured using the ImageJ software.

Detailed protocols for physiological, biochemical, molecular and cytological analyses are given in Supporting Information Methods S1. All the primers used are described in Table S1.

Results

Repression of *AtFER1* minimal promoter activity involves a *G-box cis*-regulatory sequence

To identify TFs that could link Fe deficiency and Fe excess responses, the promoter of *AtFER1* (*ProAtFER1*) was functionally characterised. The aim was to identify *cis*-regulatory sequences involved in *ProAtFER1* repression that could be used as baits in yeast one-hybrid (Y1H) screens. A deletion series of *ProAtFER1* fused to the *uidA* reporter gene (*ProAtFER1:GUS*) expressed in WT plants was carried out. This approach allowed the identification of a 496 bp minimal promoter ($ProAtFER1_{mini}$) whose activity was still inducible in response to Fe excess, as does the endogenous gene (Figs 1a, S1) (Reyt *et al.*, 2015). Sequence comparison of $ProAtFER1_{mini}$ with the corresponding sequence of *ProAtFER3* and *ProAtFER4*, the two other ferritin genes expressed in vegetative tissues (Reyt *et al.*, 2015), highlighted some potential *cis*-regulatory motifs including a *G-box* (*CACGTG*) (Fig. S2) (Strozycki *et al.*, 2010). Because most of the master TFs regulating the Fe deficiency responses belong to the bHLH family (Li *et al.*, 2016; Cui *et al.*, 2018), and because bHLH TFs bind *G-box* sequences (and more generally *E-box*, *CANNTG*) that are usually localised within the promoter of their target genes (De Masi *et al.*, 2011), this potential *cis*-regulatory element was selected for further analysis. In support of this choice, the *G-box* sequences present in the promoter of the ferritin genes were located in nucleosome-free regions (NFR), suggesting the presence of regulatory proteins at these loci when Fe is not limiting (Fig. S3).

Site-directed mutagenesis revealed that the mutation of the *G-box* (*mG-box*) leads to an enhanced $ProAtFER1_{mini}$ activity in the control (C: 50 μM Fe) condition (Fig. 1a). However, the effect of *mG-box* on $ProAtFER1_{mini}$ activity in the control condition was lower than that of the mutation of the well characterised repressive *IDRS* (*Iron-Dependent Regulatory Sequence*) regulatory element (Petit *et al.*, 2001). These observations indicate that this *G-box* plays a key role in the transcriptional repression of $ProAtFER1_{mini}$ when Fe is not in excess, and that part of the dynamic response of *AtFER1* expression to Fe availability relies on this specific *cis*-regulatory sequence.

Therefore, a 20 bp long DNA fragment containing the *G-box* (Element 5, Figs S2, S4a,b) present on $ProAtFER1_{mini}$ was used as bait for Y1H experiments using a normalised TF cDNA library (Paz-Ares, 2002). This approach led to the identification of four TFs (Fig. S4c). Among these genes, there was only one bHLH TF, *bHLH105/ILR3* (*IAA-LEUCINE RESISTANT 3*), a well described transcriptional activator of plant responses to Fe shortage (Rampey *et al.*, 2006; Zhang *et al.*, 2015; Li *et al.*, 2016). In presence of 1 mM 3-AT (3-Amino-1,2,4-triazole), ILR3 was the sole TF still interacting with the bait DNA. ILR3 interaction in Y1H experiments was abolished when the *G-box* was mutated (Fig. 1b).

ILR3 is a repressor of ferritin gene expression

To characterise the role of ILR3 in the transcriptional control of ferritin gene expression, a *ILR3* T-DNA insertion line (*ilr3-3*, knock down mutant) was studied together with another mutant expressing a dominant version of ILR3 (*ilr3-1*) and compared with WT seedlings (Fig. S5) (Rampey *et al.*, 2006; Meinke, 2013). The dominant *ilr3-1* allele displays conserved bHLH and leucine zipper domains, respectively involved in DNA binding and protein dimerisation, but lacks the C-terminal domain suspected to improve the stability of ILR3 homo- or heterodimers (Rampey *et al.*, 2006; Meinke, 2013).

Seedlings were grown with three different Fe concentrations in the growth media: control condition (C: 50 μM), Fe deficiency (−Fe: 0 μM) and Fe excess (+Fe: 500 μM). By contrast to −Fe and +Fe, C condition corresponds to Fe concentration in the culture medium allowing optimal plant growth (repleteness). qRT-PCR analysis showed that in C and +Fe conditions the mRNA steady state level of *AtFER1* was increased in the *ilr3-3* mutant when compared with WT seedlings and decreased in *ilr3-1* (Fig. 1c). In −Fe condition, *AtFER1* transcript level was increased in *ilr3-3* compared with WT seedlings, whereas no difference was observed between WT and *ilr3-1* seedlings. For the two other ferritin genes expressed in vegetative tissues, namely *AtFER3* and *AtFER4*, comparable expression patterns to that of *AtFER1* were observed (Fig. S6).

Western blot analysis confirmed that ferritin protein (FER) abundance was, in comparison with WT seedlings, higher and lower in the *ilr3-3* and *ilr3-1* mutants, respectively (Fig. 1d). Under C conditions, the difference in *AtFER1* transcript levels between WT and *ilr3-3* was less pronounced when compared with the difference observed at the protein levels. Since the antibody used recognises all three ferritins, this observation suggests that ILR3 might regulate AtFER1 and/or AtFER3 and AtFER4 protein abundance through a mechanism that expands beyond the sole regulation of their expression.

Then, WT plants carrying the $ProAtFER1_{mini}$*:GUS* and $ProAtFER1_{mini}$*-mG-box:GUS* constructs were crossed with the *ilr3-3* and *ilr3-1* mutants. Homozygous mutant plants harbouring the transgenes were selected, and the GUS activities analysed (Fig. 1e). As expected, $ProAtFER1_{mini}$*:GUS* activity led to a more intense blue coloration in *ilr3-3* mutant when compared with both WT and *ilr3-1*. This result highlighted the repressive role of ILR3 on the activity of $ProAtFER1_{mini}$. $ProAtFER1_{mini}$*-mG-box:*

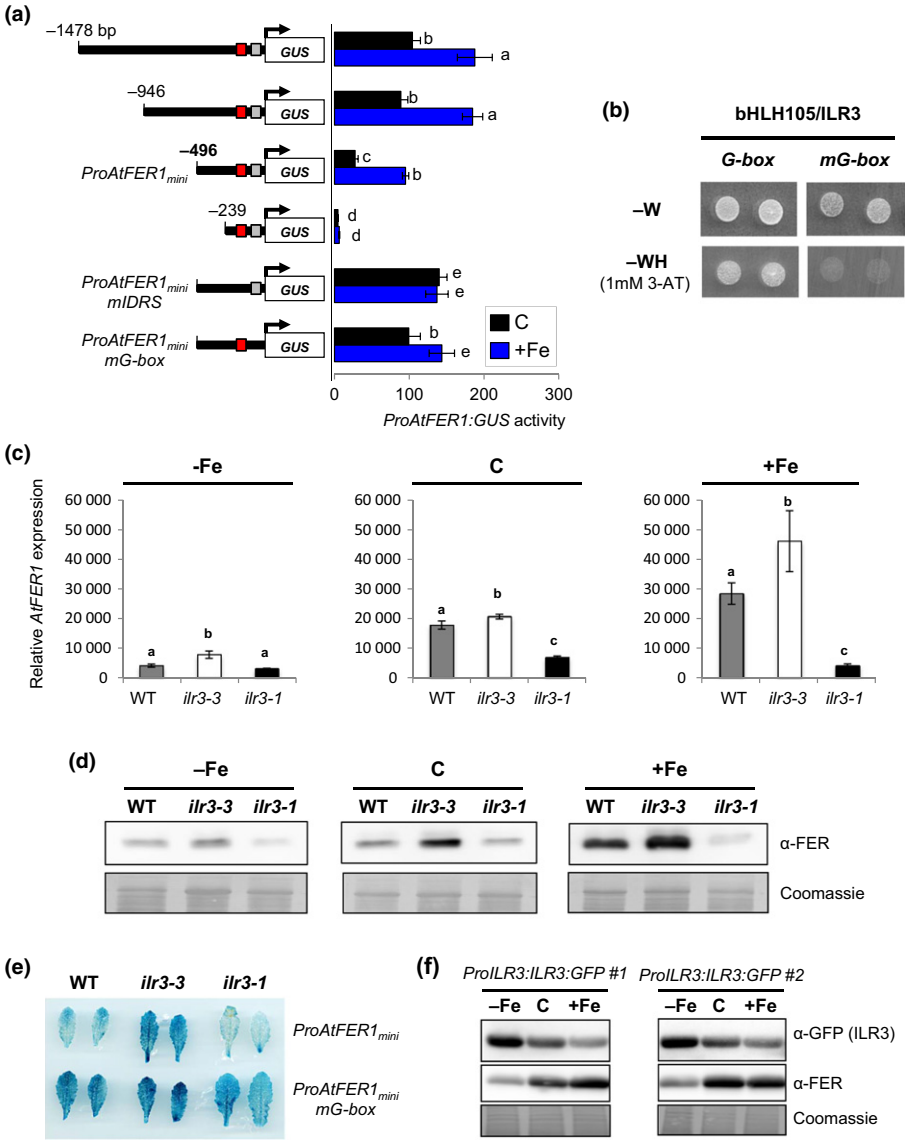

Fig. 1 ILR3 is a repressor of ferritin genes expression. (a) Left panel, scheme of 5′-end deletion and site-directed mutagenesis constructs used for the functional characterisation of *ProAtFER1* as revealed by GUS (β-glucuronidase) activity in 2-wk-old wild-type (WT) *Arabidopsis thaliana* seedlings. Red boxes, *IDRS* (*AGCACGAGGCCGCCACACGCCCC*); grey boxes, *G-box* (*CACGTG*). *mIDRS*, mutated *Iron-Dependent Regulatory Sequence*; *mG-box*, mutated *G-box cis*-regulatory sequence. C and +Fe correspond to the control (50 μM Fe) and Fe excess (500 μM Fe) condition, respectively. Right panel, quantitative GUS analysis (nmol 4-MU min^{-1} mg^{-1} proteins) driven by *ProAtFER1* 5′-end deletion and site-directed mutagenesis constructs. Means with the same letter are not significantly different according to one-way analysis of variance (ANOVA) followed by post-hoc Tukey test, $P < 0.05$ ($n = 6$, three biological repeats × 2 independent transgenic lines, from one representative experiment). Error bars show ± SD. (b) Yeast one-hybrid experiment: yeasts were stably transformed with tetramers of a 20 bp long *ProAtFER1* DNA fragment containing the native *G-box* or a mutated version (*mG-box*) fused to *HIS3* (auxotrophic markers). These two yeast strains were then transfected with ILR3/bHLH105. Upper panel, growth on control media deprived of W amino acids. Lower panel, growth on selective media deprived of W and H amino acids. 3-AT, 3-amino-1,2,4-triazole. Two independent colonies per construct are shown. (c) Quantitative RT-PCR (qRT-PCR) analysis of *AtFER1* mRNA levels in 2-wk-old WT, *ilr3-3* (loss-of-function) and *ilr3-1* (dominant mutation) seedlings. −Fe, C and +Fe correspond to Fe deficiency (0 μM Fe), control (50 μM Fe), and Fe excess (500 μM Fe) condition, respectively. Means with the same letter are not significantly different according to one-way ANOVA followed by post-hoc Tukey test, $P < 0.05$ ($n = 3$ biological repeats from one representative experiment). Error bars show ± SD. (d) Abundance of ferritin proteins in 2-wk-old WT, *ilr3-3* and *ilr3-1* seedlings grown as in (a). (e) Histochemical detection of GUS activity driven by the $ProAtFER1_{mini}$ with the native or the mutated *G-box* (*mG-box*) in WT, *ilr3-3* and *ilr3-1* leaves. (f) Western blot analysis of ILR3 (α-GFP) and ferritin proteins (α-FER) in 2-wk-old WT seedlings expressing *pILR3::gILR3:GFP* (2 independent transgenic lines are shown, #1 and #2) grown as in (c).

GUS staining was stronger in all three genotypes tested when compared with WT plants expressing $ProAtFER1_{mini}$:*GUS*, confirming the role of the *G-box* in the repression of $ProAtFER1_{mini}$ activity. This experiment demonstrates, *in planta*, the genetic connection between ILR3 and the *G-box* present in $ProAtFER1_{mini}$.

Because of the repressive role of ILR3 on *AtFER1* expression, one would expect that a negative correlation exists *in planta* in term of protein accumulation between ILR3 and the FER proteins. Western blot analysis was carried out using WT plants expressing the *ProILR3:gILR3:GFP* construct. This experiment confirmed the negative correlation between ILR3 abundance and Fe availability (Fig. 1f).

In order to determine if ILR3 function in regulating ferritin gene expression is unique within the bHLH clade it belongs to (IVc), *AtFER1* mRNA abundance was measured in *bhlh34*, *bhlh104* and *bhlh115* loss-of-function mutants (Zhang *et al.*, 2015; Li *et al.*, 2016). No variation in *AtFER1* expression was found in *bhlh34*, *bhlh104* and *bhlh115* mutants when compared with WT seedlings for the three Fe conditions tested, by contrast to what is observed for the *ilr3-3* mutants (Fig. S7).

Taken together, these data demonstrate that ILR3 repression of ferritin gene expression is specific within the clade IVc bHLHs.

ILR3 acts as both transcriptional activator and repressor to regulate Fe homeostasis

To determine if ILR3 repressive activity is specific to the ferritin genes, mRNA abundance of genes associated with Fe homeostasis and/or metabolism was measured by qRT-PCR under contrasting Fe conditions (C, −Fe and +Fe).

APX1 is strongly induced in response to Fe excess and encodes the cytosolic ASCORBATE PEROXIDASE 1 that is, with the ferritin genes, another well known marker of the Arabidopsis response to Fe excess (Fourcroy *et al.*, 2004). *APX1* mRNA abundance was unaffected in the *ilr3-1* and *ilr3-3* mutant backgrounds when compared with WT seedlings regardless of the Fe condition (Fig. S8a). This observation indicates that the regulation of ferritin expression by ILR3 is related to the control of Fe homeostasis *per se*. As expected, *IRT1* expression was diminished in *ilr3-3* when compared with WT and *ilr3-1* seedlings in response to −Fe (Fig. S8b; Zhang *et al.*, 2015). By contrast, *IRT1* mRNA level was higher in *ilr3-1* when compared with WT seedlings in C or +Fe conditions. Because *bHLH39* is a known target of ILR3 that participates to the transcriptional regulation of *IRT1* expression in response to Fe shortage (Zhang *et al.*, 2015), its mRNA steady state level was also analysed. This analysis confirmed that *bHLH39* expression is induced in response to −Fe in an ILR3-dependent manner (Fig. S8c). Last, *NAS4* expression was increased in *ilr3-3* when compared with WT and *ilr3-1* seedlings in −Fe or C conditions (Fig. 2a). These data indicate that ILR3, like PYE, represses *NAS4* expression when Fe is not in excess.

Three additional genes whose expression was previously reported to depend on ILR3 activity were assayed, namely *At-NEET*, *VTL2* (*VACUOLAR IRON TRANSPORTER-LIKE 2*) and *PYE*. *At-NEET* encodes a protein that is capable of transferring [Fe-S] cluster to an acceptor protein and that is thought to play a role in Fe homeostasis and/or metabolism (Nechushtai *et al.*, 2012). As previously described, *At-NEET* mRNA abundance was decreased in *ilr3-1* and unaffected in *ilr3* loss-of-function mutant when compared with WT seedlings grown in C condition (Fig. 2b) (Rampey *et al.*, 2006). Surprisingly, growth in −Fe or +Fe conditions led to a drastic decrease of *At-NEET* mRNA abundance in both mutants when compared with WT seedlings. These observations indicate that ILR3 represses *At-NEET* expression when plants are grown under Fe-replete condition. *VTL2* encodes a Fe vacuolar transporter whose expression was previously reported as increased in *ilr3-1* and decreased in *ilr3* loss-of-function mutant when compared with WT seedlings (Gollhofer *et al.*, 2011, 2014). This pattern of *VTL2* mRNA accumulation was conserved regardless of the Fe concentration in which seedlings were grown, with a less marked difference between WT and *ilr3-3* in +Fe condition (Fig. 2c). These data confirm that, like for the ferritin genes, ILR3 is a transcriptional repressor of *VTL2* expression. *PYE* mRNA abundance was then measured as PYE was proposed to be a target of ILR3

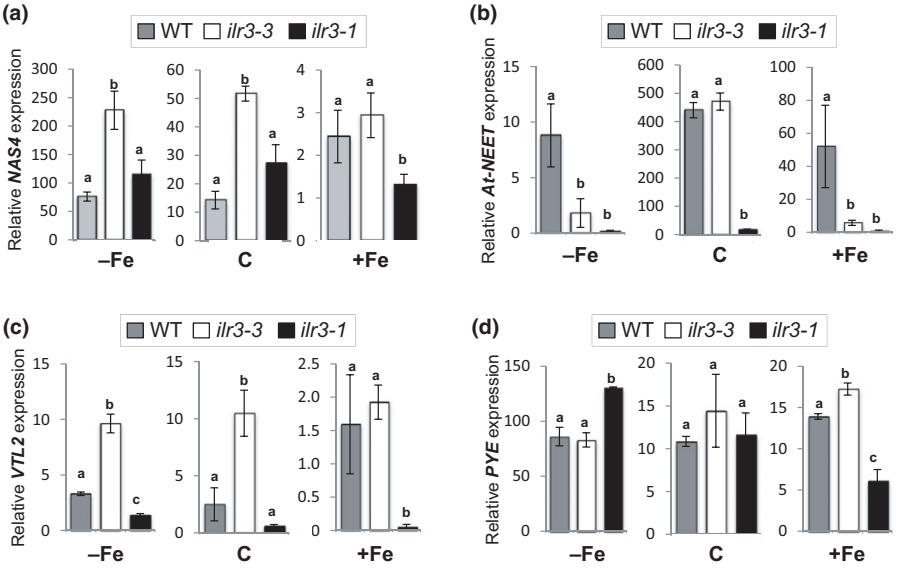

Fig. 2 ILR3 acts as both transcriptional activator and repressor to regulate Fe homeostasis. Relative expression of (a) *NAS4* (*NICOTIANAMINE SYNTHASE 4*), (b) *At-NEET*, (c) *VTL2* (*VACUOLAR IRON TRANSPORTER-LIKE 2*) and (d) *PYE* (*POPEYE/bHLH47*) genes as revealed by quantitative RT-PCR analysis in 2-wk-old *Arabidopsis thaliana* wild type (WT), *ilr3-1* and *ilr3-3* seedlings. −Fe, C and +Fe correspond to Fe deficiency (0 μM Fe), control (50 μM Fe), and Fe excess (500 μM Fe) conditions, respectively. Means within each condition with the same letter are not significantly different according to one-way ANOVA followed by post-hoc Tukey test, $P < 0.05$ ($n = 3$ biological repeats from one representative experiment). Error bars show ± SD.

(Zhang *et al.*, 2015; Li *et al.*, 2016). This analysis revealed that *PYE* expression was higher in the *ilr3-1* mutant when compared with WT and *ilr3-3* in −Fe condition, confirming the positive role of ILR3 on *PYE* expression when Fe availability is low (Fig. 2d). By contrast, when Fe availability was not limiting, *PYE* expression appeared to be repressed in an ILR3-dependent manner, in particular in the +Fe condition. This later observation suggests that ILR3 acts as a transcriptional repressor of *PYE* expression when Fe is not limiting.

ILR3 binds to *E-box* motifs present in the promoter of its target genes

In order to determine whether or not ILR3 interacts with the *E-box* motifs present in the promoter of the ferritins genes (*AtFER1*, *AtFER3* and *AtFER4*), as well as with the promoter of *At-NEET*, *VTL2* and *NAS4*, ChIP experiments were carried out (Fig. 3a). ChIP experiments were conducted on two independent transgenic lines expressing the *ProILR3:gILR3:GFP* construct using an anti-GFP antibody (Figs 1f, S9). A promoter fragment containing an *E-box* motif for both *bHLH39* and *FIT* was used as positive and negative control, respectively (Zhang *et al.*, 2015). As previously reported, ChIP-qPCR analyses showed that ILR3 bound to the promoter of *bHLH39* (*ProbHLH39*) and not to the one of *FIT* (*ProFIT*) (Fig. 3b). The results presented Fig. 3c–e support the *in vivo* binding of ILR3 to the promoter of *AtFER1* (*ProFER1*), *AtFER3* (*ProFER3*) and *AtFER4* (*ProFER4*) with a higher affinity to the regions that contain the canonical *E-box* motif *CACGTG* also called *G-box* (Figs 1b, 3c–e). ILR3 also bind to the promoter of *At-NEET* (*ProAt-NEET*), *VTL2* (*ProVTL2*) and *NAS4* (*ProNAS4*) (Fig. 3f–h). Interestingly, ILR3 interacts with *ProNAS4* at the same locus than PYE, located on the main NFR region of *ProNAS4* that is about 3.2 kb upstream from the transcriptional initiation start (Fig. S10) (Long *et al.*, 2010).

These results indicate that ILR3 interacts with specific *E-box* motifs present in the promoter of its target genes to affect their transcription, in accordance with the amount of Fe that is present in the surrounding media.

ILR3 and PYE repress the expression of a common set of genes

mRNA abundance of genes whose expression is repressed by ILR3 was measured in loss-of-function *pye-1* mutant grown by contrasting Fe conditions (−Fe, C and +Fe) and compared with that of WT seedlings. *AtFER1*, *AtFER3* and *AtFER4* expression was induced in *pye-1* mutant regardless of the Fe condition in which seedlings were grown (not significantly for *AtFER1* in C

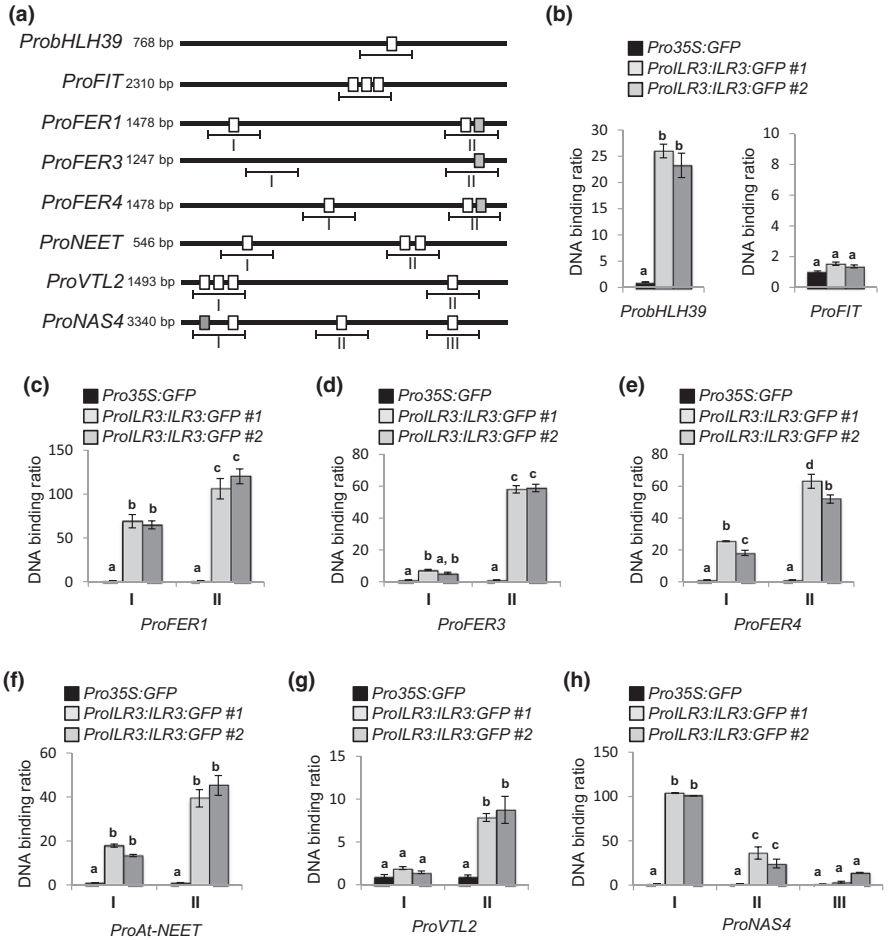

Fig. 3 Chromatin immunoprecipitation (ChIP)-qPCR analysis of the binding of ILR3 to the promoter of selected Fe deficiency or excess responsive genes. (a) Promoter structure diagrams for the assayed genes. White boxes, *E-box* (*CANNTG*); grey boxes, *G-box* (*CACGTG*). Lines under the boxes indicate sequences detected by ChIP-qPCR assays. Chromatin from 2-wk-old wild-type *Arabidopsis thaliana* seedlings expressing *ProILR3:gIL3:GFP* (two independent transgenic lines) and grown under Fe deficiency was extracted using anti-GFP antibodies. Seedlings overexpressing GFP (*Pro35S:GFP*) were used as a negative control. qPCR was used to quantify enrichment of ILR3 to the selected gene promoters. Means within each condition with the same letter are not significantly different according to one-way ANOVA followed by post-hoc Tukey test, $P < 0.05$ ($n = 3$ technical repeats from one representative experiment). Error bars show ± SD. (b) ILR3 DNA binding ratio (as revealed by GFP enrichment in ChIP experiments) to the promoter of *bHLH39* and *FIT* used as the positive or negative control, respectively (Zhang *et al.*, 2015). ILR3 binding ratio to the promoter of (c) *AtFER1*, (d) *AtFER3*, (e) *AtFER4*, (f) *At-NEET*, (g) *VTL2* and (h) *NAS4*.

condition), indicating that PYE acts as a transcriptional repressor of ferritin genes expression (Figs 4a, S11a,b). Similarly, *At-NEET*, *VTL2* and *NAS4* mRNA levels were increased in *pye-1* when compared with WT seedlings when grown in −Fe and C conditions. These observations indicate that PYE is a repressor of *At-NEET*, *VTL2* and *NAS4* expression when Fe is not in excess (Fig. 4b,d). By contrast, *ILR3* expression in *pye-1* mutant was unaffected when compared with WT seedlings regardless of the Fe condition, supporting the postulate that PYE is not a transcriptional regulator of *ILR3* expression (Fig. S11c).

ChIP experiments were then conducted on a transgenic line expressing the *ProPYE:gPYE:GFP* (in *pye-1*) using an anti-GFP antibody (Fig. 4e–j) (Long *et al.*, 2010). This approach revealed that PYE interacts *in planta* with the same promoter loci than ILR3 on *ProFER1*, *ProFER3*, *ProFER4*, *ProAt-NEET*, *ProVTL2* and *ProNAS4*. Since ILR3 could potentially act as a transcriptional repressor of *PYE* expression when Fe is not limiting (Fig. 2d), additional ChIP experiments were conducted in order to determine if ILR3 and PYE interact at the same locus with the promoter of *PYE*. For this purpose, the above described *ProILR3:gILR3:GFP* (positive control; Zhang *et al.*, 2015) and *ProPYE:gPYE:GFP* transgenic lines were used revealing that PYE can interact with its own promoter at the same locus than ILR3 (Fig. 5a,b).

Altogether, these experiments show that ILR3 and PYE repress the expression of a common set of genes (for example *AtFER1*, *AtFER3*, *AtFER4*, *VTL2*, *At-NEET* and *NAS4*) and that the transcriptional repressor activity of ILR3 is likely conferred by its heterodimerisation with PYE (Long *et al.*, 2010). This later hypothesis is supported by BiFC experiments that show, *in planta*, the nuclear localisation of ILR3 and PYE interaction *in planta* (Fig. 5c) (Zhang *et al.*, 2015).

ILR3 and ferritin activities modulate Arabidopsis growth in a Fe-dependent manner

WT, *ilr3-3*, *pye-1*, *ilr3-3 pye-1*, and *ilr3-1* seedlings were grown under contrasting Fe concentrations in order to determine if ILR3 activity could affect seedling growth in a Fe-dependent manner. In −Fe condition a strong reduction of *ilr3-3*, *pye-1*, and *ilr3-3 pye-1* root growth was observed when compared with WT seedlings, confirming observations made in previous studies (Fig. S12a,d) (Zhang *et al.*, 2015; Li *et al.*, 2016). Among the three mutants, *pye-1* was the less affected whereas *ilr3-3 pye-1*

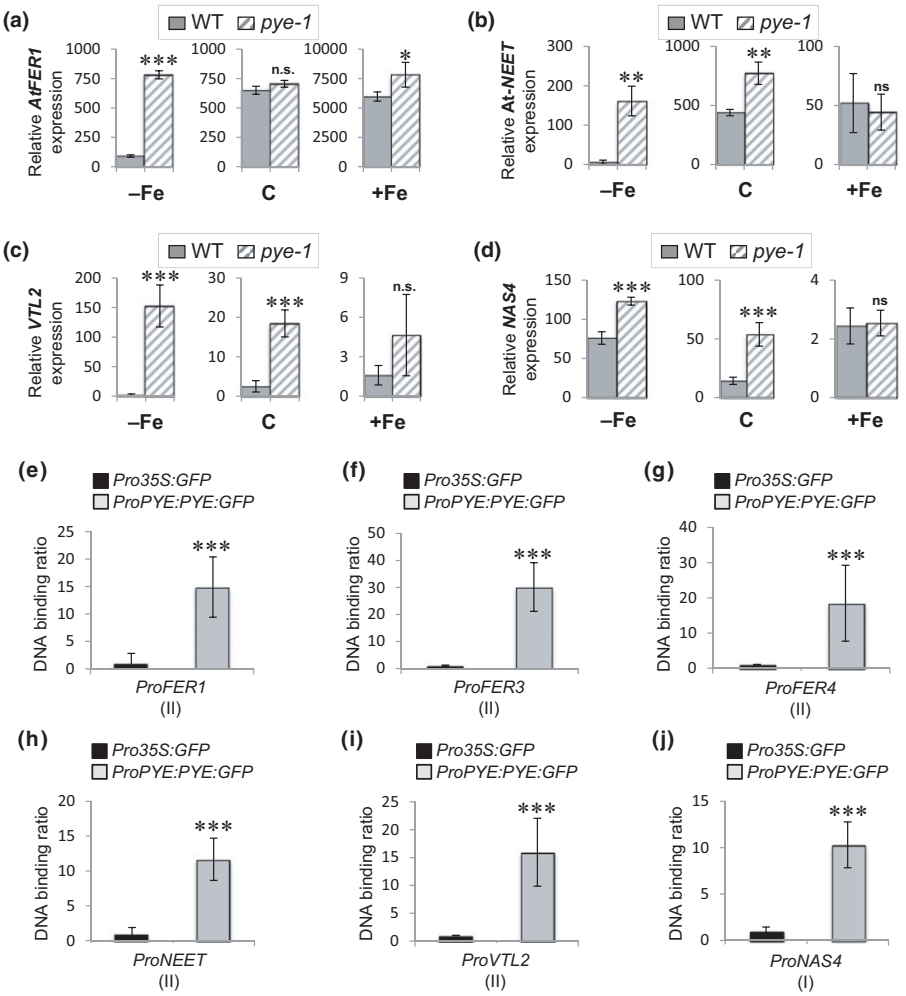

Fig. 4 ILR3 and PYE regulate common set of genes. Relative expression (qRT-PCR) of (a) *AtFER1*, (b) *At-NEET*, (c) *VTL2* and (d) *NAS4* genes as revealed by quantitative RT-PCR analysis in 2-wk-old *Arabidopsis thaliana* wild-type (WT) and *pye-1* seedlings. −Fe, C and +Fe correspond to the control (50 μM Fe), Fe deficiency (0 μM Fe) and Fe excess (500 μM Fe) conditions, respectively. *t*-test significance (compared with WT): *, $P < 0.05$; **, $P < 0.01$; ***, $P < 0.001$, ns not significant. Error bars show ± SD. (e–j) Chromatin immunoprecipitation (ChIP)-qPCR analysis of the binding of PYE to the promoter of selected genes whose expression is repressed by ILR3. Chromatin from 2-wk-old Arabidopsis seedlings expressing *ProPYE:PYE:GFP* (Long *et al.*, 2010) and grown under Fe deficiency was extracted using anti-GFP antibodies. Seedlings overexpressing GFP (*Pro35S:GFP*) were used as the negative control. qPCR was used to quantify enrichment of PYE to promoter regions that are targeted by ILR3 (Fig. 3). PYE DNA binding ratio (as revealed by GFP enrichment in ChIP experiments) to the promoter of (e) *AtFER1*, (f) *AtFER3*, (g) *AtFER4*, (h) *At-NEET*, (i) *VTL2* and (j) *NAS4*. *t*-test significance: ($n = 2$ technical repeats from one representative experiment) ***, $P < 0.001$; ns, not significant. Error bars show ± SD.

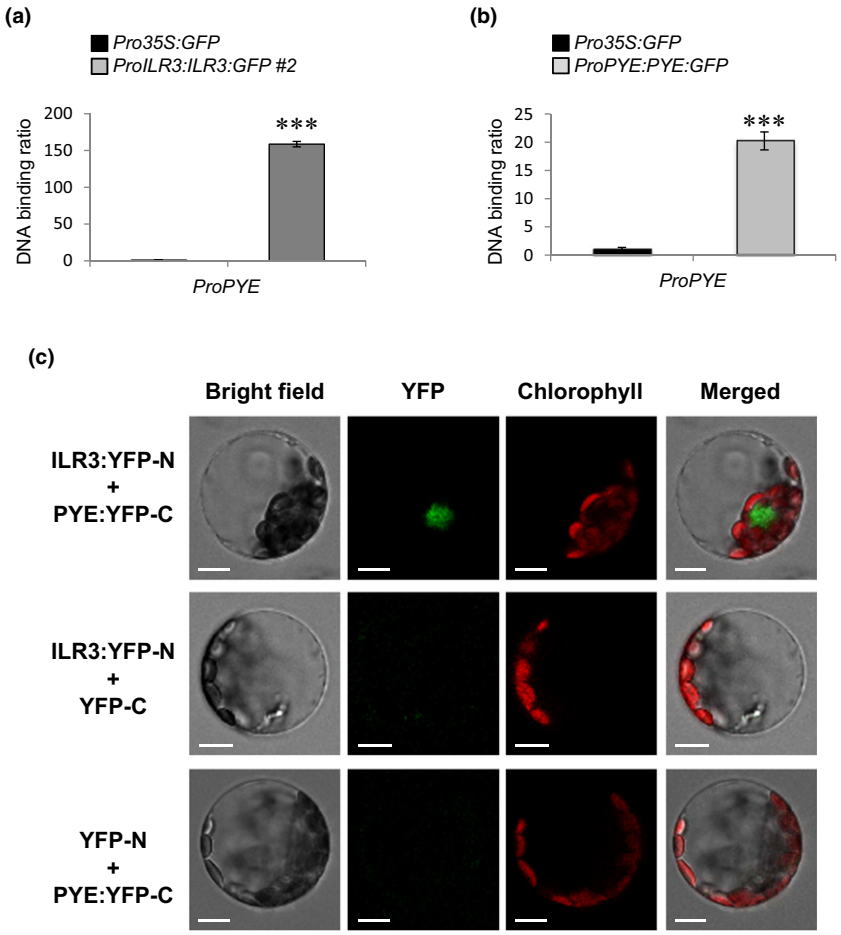

Fig. 5 ILR3 and PYE directly interact, at the same locus, on *PYE* promoter. (a, b) Chromatin immunoprecipitation (ChIP)-qPCR analysis of the binding of ILR3 and PYE to the promoter of *PYE* (*ProPYE*). Chromatin from 2-wk-old wild-type (WT) *Arabidopsis thaliana* seedlings expressing *ProILR3:ILR3:GFP* or *ProPYE:PYE:GFP* (Long *et al.*, 2010) and grown under Fe deficiency was extracted using anti-GFP antibodies. Seedlings overexpressing GFP (*Pro35S:GFP*) were used as the negative control. qPCR was used to quantify enrichment of ILR3 and PYE to *PYE* promoter region that is targeted by ILR3 (Zhang *et al.*, 2015). ILR3 and PYE DNA binding ratio (as revealed by GFP enrichment in ChIP experiments) to the promoter *PYE* are presented in (a) and (b), respectively. *t*-test significance: ($n = 3$ technical repeats from one representative experiment) ***, $P < 0.001$. Error bars show ± SD. (c) Bimolecular fluorescence complementation labelled ILR3-PYE complexes in *Arabidopsis thaliana* protoplasts. Bars, 10 μm.

displayed a similar phenotype to that of *ilr3-3*. Conversely, an opposite trend was observed for the *ilr3-1* mutant. Under Fe-replete condition, no significant difference in root length was observed between the mutants and WT seedlings (Fig. S12b,e). When seedlings were grown on Fe excess, root growth was drastically affected in all six genotypes. However, *ilr3-3*, *pye-1* and *ilr3-3 pye-1* on one hand and *ilr3-1* on the other displayed longer and shorter root length when compared with WT seedlings, respectively (Fig. S12c,f). Similarly to root growth, seedling fresh weight was also affected in a Fe-dependent manner (Fig. S13). These data suggest that ILR3 function extends beyond its role in the control of plant response to −Fe to a more central role in the transcriptional regulation of plant growth in response to Fe availability.

To investigate the possibility that the role of ILR3 in the Fe-dependent control of seedlings growth may involve ferritin activity, the triple *fer1,3,4* ferritin loss-of-function mutant was included in the analysis. Growth parameters of the *fer1,3,4* mutant were compared with those of the *ilr3-3*, *pye-1*, *ilr3-3 pye-1* and *ilr3-1* mutants and WT seedlings (Fig. S12). In all the conditions tested, the *fer1,3,4* and the *ilr3-1* mutants displayed similar growth parameters when compared with WT seedlings. These later observations suggest that part of ILR3 function relies on ferritin activity. In order to test this hypothesis, *ilr3-1* mutant overexpressing *AtFER1* lines (*Pro35S:FER1*) were generated and grown as described above (Figs 6, S14). This approach revealed that the overexpression of *AtFER1* in *ilr3-1* was sufficient to revert the *ilr3-1* seedling root length and fresh weight phenotypes. Importantly, under Fe-replete condition, no significant difference was observed between the different genotypes. Altogether these experiments indicate that part of ILR3 function in the control of seedling growth, in response to Fe availability, relies on ferritin activity. Additional experiments also revealed that ILR3, by modulating ferritin expression, plays a key role in the response to Fe availability not only in seedlings but also in adult plants (Figs S15, S16).

ILR3 and PYE regulate Fe distribution in leaves

To characterise ILR3's role in the control of Fe homeostasis, Fe accumulation in rosette leaves was evaluated.

First, the Fe content present in the leaves of 6-wk-old plants grown under three different conditions was measured: Fe-replete condition (C, 50 μM), Fe deficiency (−Fe: 20 d of Fe deficiency prior harvesting) and Fe excess (+Fe: 10 d of Fe deficiency followed by 10 d of Fe excess prior harvesting) (Fig. S17). This experiment revealed, for all genotypes, that the Fe content increased as the amount of Fe in the media rose. Under −Fe condition, no significant difference in Fe content was observed between the different genotypes. Under Fe-replete condition,

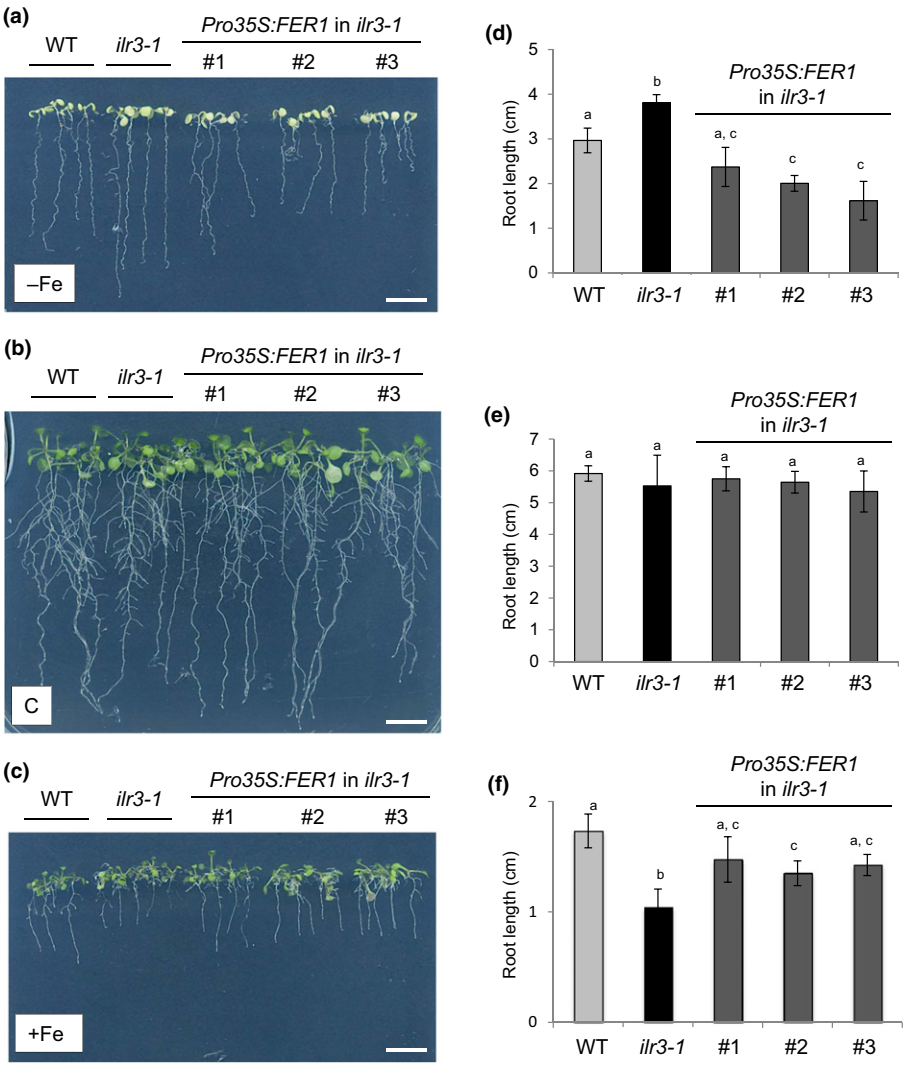

Fig. 6 Complementation of *ilr3-1* seedling root growth phenotypes by overexpressing *AtFER1*. Seedling phenotypes of the wild-type (WT), *ilr3-1* and three independent *ilr3-1* lines overexpressing *AtFER1* (*Pro35S:FER1* in *ilr3-1*) grown for 2 wk in (a) Fe deficiency (0 μM Fe), (b) control (50 μM Fe), and (c) Fe excess (500 μM Fe) conditions. Bar, 1 cm. Root length of WT, *ilr3-1* and three independent *ilr3-1* lines overexpressing *AtFER1* (*Pro35S:FER1* in *ilr3-1*) grown for 2 wk in (d) Fe deficiency (0 μM Fe), (e) control (50 μM Fe), and (f) Fe excess (500 μM Fe) conditions. Means within each condition with the same letter are not significantly different according to one-way ANOVA followed by post-hoc Tukey test, $P < 0.05$ ($n = 16$ seedlings from one representative experiment). Error bars show ± SD.

ilr3-1 mutant accumulated more Fe than any other genotype. This later observation was more pronounced in Fe excess.

Fe localisation in leaves of 5-wk-old WT, *ilr3-3*, *pye-1*, *ilr3-3 pye-1* and *ilr3-1* plants grown in soil and watered or not with an excess of Fe was then determined (Fig. 7). For this purpose, the Perls/DAB histochemical staining method was used (Roschzttardtz *et al.*, 2009, 2013). *ilr3-3*, *pye-1* and *ilr3-3 pye-1* Perls/DAB staining was similar to that of WT plants but displayed some more Fe-rich structures (black dots), in particular alongside the vasculature (that is vascular bundle and mesophyll cells) where the ferritins accumulate when Fe availability is in excess (Roschzttardtz *et al.*, 2013). Interestingly, these Fe-rich dots are absent in *ilr3-1*. Instead, Fe accumulates in plaques in the vascular bundle and is nearly totally absent from the mesophyll cells. The absence of Fe-rich dots in *ilr3-1* is in agreement with the lack of induction of ferritin genes expression in response to Fe excess in this mutant as these structures are described as being Fe-ferritin (Roschzttardtz *et al.*, 2013). In addition, these data support the hypothesis that ferritins play an important role in buffering the excess of Fe during xylem unloading (Roschzttardtz *et al.*, 2013).

Taken together, these data highlight that ILR3 regulates, in addition to Fe uptake, the distribution of Fe at the tissue, cellular and subcellular levels.

Discussion

ILR3/bHLH105 is a transcriptional regulator of ferritin genes expression

The ferritins are a class of ubiquitous Fe storage proteins found in all living kingdoms and that play a central role in the control of Fe homeostasis (Briat *et al.*, 2010). In plants, the role of ferritins is to buffer Fe to maintain Fe concentration to levels that are optimal for metabolic purposes and to avoid the deleterious effects of free Fe-associated reactive oxygen species (ROS) (Ravet *et al.*, 2009). The abundance of ferritins found in plants (mostly in chloroplasts) is transiently induced in response to Fe excess. The induction of ferritin mRNA levels is essentially regulated at the transcriptional level and involves the *cis*-regulatory element *IDRS* (*Iron-Dependent Regulatory Sequence*) through which ferritins expression is repressed (Petit *et al.*, 2001). No *trans*-acting

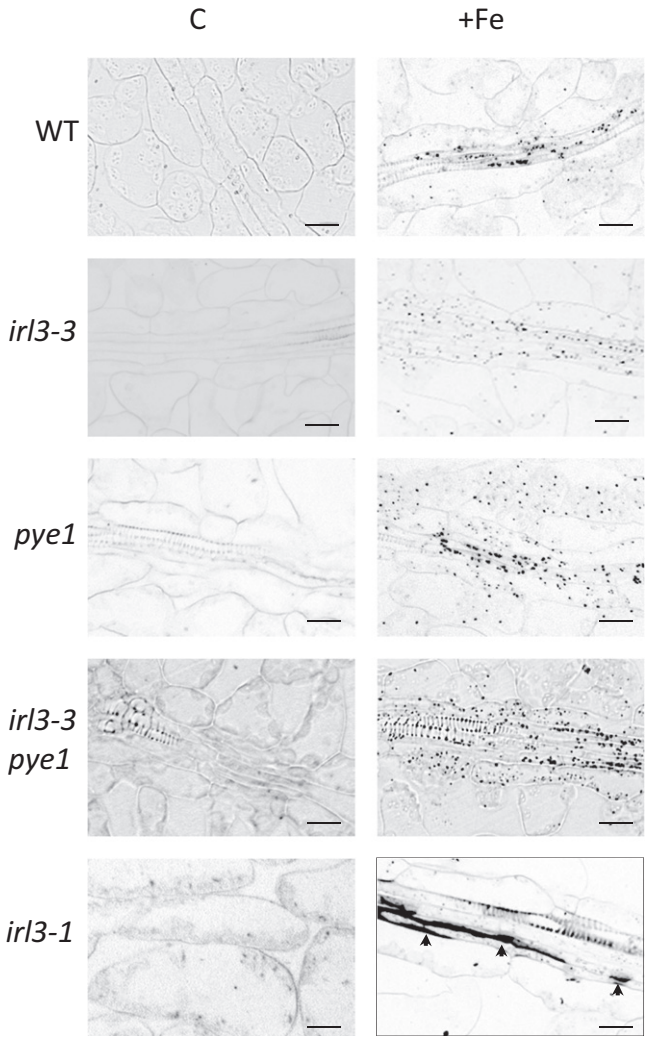

Fig. 7 ILR3 regulates Fe storage in leaves. Fe localisation in rosette leaves as revealed by Perls/DAB histochemical staining of *Arabidopsis thaliana* wild-type (WT), *ilr3-3*, *pye-1*, *ilr3-3 pye-1* and *ilr3-1* plants grown in control (left panels, C) or Fe excess condition (right panels, +Fe). Arrows, Insoluble iron in vasculature; bars, 20 μm.

factors interacting with the *IDRS* have been identified so far. Strikingly, all the studies aiming at decrypting the molecular mechanisms controlling ferritins expression have failed in identifying any actor repressing ferritin gene expression in response to Fe deprivation. Instead, it has been found that Fe is not the sole signal that directly modulates ferritin genes expression. Ferritin gene expression is under the control of the circadian clock and involves the nuclear factor TIC (TIME FOR COFFEE) (Fourcroy *et al.*, 2004; Duc *et al.*, 2009). Plant ferritin gene expression is also tightly connected to phosphate availability. In Arabidopsis, *AtFER1* expression (the most expressed ferritin gene present in vegetative tissues) is induced under phosphate starvation (Briat *et al.*, 2010; Bournier *et al.*, 2013). This induction relies on the interaction between two MYB-like TFs (PHOSPHATE STARVATION RESPONSE 1, PHR1 and PHR1-like 1, PHL1) and the *P1BS* (*PHR1 binding site*) *cis*-regulatory sequence present on *AtFER1* promoter. An *AtFER1* promoter-based strategy was therefore developed with the aim to identify key molecular players that could coordinate the transcriptional regulatory cascade associated with the Fe acquisition from the soil and the Fe buffering activity of ferritins, connecting the plant responses to Fe deficiency and Fe excess. This approach led to the identification of both a *cis*-regulatory motif (*G-box*) through which *AtFER1* expression is repressed, and a cognate *trans*-acting factor, namely bHLH105/ILR3 (IAA-LEUCINE RESISTANT 3) (Fig. 1). ILR3 binding to this *G-box* was then confirmed *in planta* by ChIP experiments (Fig. 3) and its repressive role on *AtFER1* expression was validated using dominant (*ilr3-1*) and loss-of-function (*ilr3-3*) mutant alleles (Fig. 1). Importantly, ILR3 has been described as a master regulator of the plant responses to Fe shortage acting as a transcriptional activator (Zhang *et al.*, 2015; Li *et al.*, 2016). Therefore, it emerges that the role of ILR3 extends beyond the activation of the Fe acquisition machinery in response to Fe deficiency. Indeed, it connects the plant responses to both Fe deficiency and Fe excess, which are of central importance when plants are recovering from a period of Fe shortage or when Fe availability in the soil solution is fluctuating.

ILR3 integrates Fe signals to adjust plant growth

The transcriptional activity of ILR3 in coordinating the responses to Fe shortage is central for the plant survival. The ILR3-dependent transcriptional regulatory cascade is well characterised and most of the downstream targets participating to Fe assimilation from the soil by the plant have been identified (Brumbarova *et al.*, 2015; Li *et al.*, 2016). The specific role of ILR3 in the context of Fe deficiency is best exemplified by the extent of the growth defects that are observed in *ilr3-3* mutant when compared with WT plants (Figs S12, S13) (Zhang *et al.*, 2015; Li *et al.*, 2016). These growth defects are abolished in plants displaying increased ILR3 activity (*ilr3-1*). Nevertheless, some evidence suggests that ILR3 function may extend beyond the induction of the sole Fe acquisition machinery. ILR3 was first characterised as a potential regulator of metal homeostasis and (auxin) IAA-conjugate metabolism, whose activity was dependent on Fe availability (Rampey *et al.*, 2006). Rampey *et al.* (2006) found that ILR3 may regulate the expression of three vacuolar Fe transporter homologues (Gollhofer *et al.*, 2011, 2014) and a gene encoding a chloroplastic [Fe–S] cluster transfer protein called At-NEET (Nechushtai *et al.*, 2012). A recent study showed that ILR3 is involved in the salicylic acid-dependent defence signalling response in *Arabidopsis* and that ILR3 acts as transcriptional regulator of *At-NEET* expression (Aparicio & Pallas, 2016). Importantly, plant sensitivity to Fe availability is also dependent on At-NEET activity as its suppression renders mutant plants more susceptible to Fe deprivation and more resistant to Fe excess than WT plants (Nechushtai *et al.*, 2012). By contrast to its role in response to Fe deficiency, our data indicate that ILR3 functions as a repressor of the plant responses to high Fe concentrations, in agreement with an increased sensitivity of the *ilr3-1* mutant to an excess of Fe compared with WT plants (Figs S12, S13). Interestingly, it has recently been shown that ILR3 acts as a

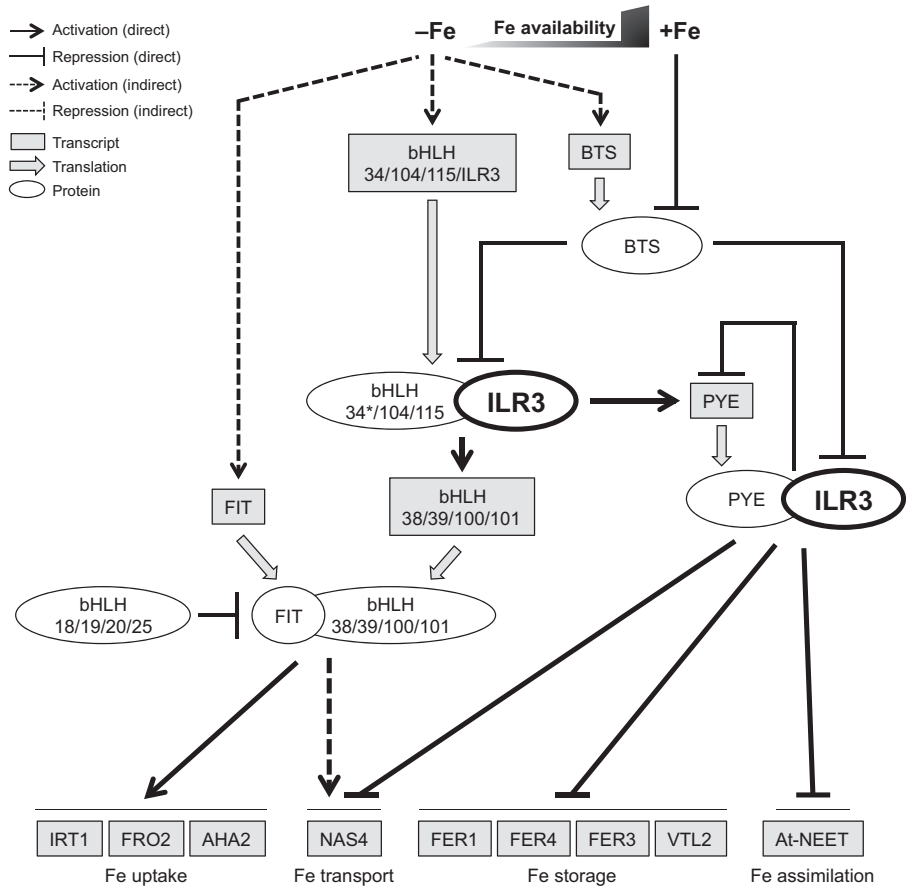

Fig. 8 ILR3-mediated control of Fe homeostasis. The proposed model describes the dual role played by ILR3/bHLH105 in the control of the plant responses to fluctuations in Fe availability present in the growth medium. Depending on its interacting partner ILR3 acts as a transcriptional activator or repressor. Activating ILR3-dependent complexes relies on ILR3 heterodimerisation with bHLH34, bHLH104 and bHLH115. ILR3 as well as bHLH34, bHLH104 and bHLH115 belong to the bHLH clade IVc. ILR3 repressing activity relies on its heterodimerisation PYE/bHLH47 (clade IVb; Long *et al.*, 2010). PYE expression as well as expression of additional bHLH transcription factors regulating the plant response to Fe shortage (for example *bHLH39*, clade Ib) depends on activating ILR3-dependent complexes (Zhang *et al.*, 2015). A negative feedback regulatory loop involving the ILR3-PYE complex might repress the expression of *PYE* when Fe availability is not limiting. FIT/bHLH29 is another key transcriptional regulator of the plant response to Fe deficiency whose activity modulates the expression of structural or regulatory genes (for example *MYB10* and *MYB72*) required to maintain Fe homeostasis (Palmer *et al.*, 2013; Wang *et al.*, 2007, 2013). Part of FIT activity relies on its ability to form heterodimers with some clade Ib bHLH TFs (that is bHLH38, bHLH39, bHLH100 and bHLH101), and its stability is affected by its interaction with clade IVa bHLH TFs (that is bHLH18, bHLH19, bHLH20 and bHLH25) (Cui *et al.*, 2018). Structural genes whose expression is modulated by ILR3 are involved in Fe acquisition (for example *IRT1*, *FRO2*, *AHA2*), transport (for example *NAS4*), storage (for example *AtFER1*, *AtFER3*, *AtFER4*, *VTL2*) and assimilation (for example *At-NEET*). ILR3-dependendent activities are modulated by the activity of BTS (BRUTUS; Selote *et al.*, 2015; Matthiadis & Long, 2016), an E3 ubiquitin ligase that specifically targets clade IVc bHLH transcription factors leading to their degradation through the 26S proteasome (*, excluding bHLH34). BTS expression is induced in response to Fe deficiency in order to fine tune Fe uptake and avoid Fe excess that could be detrimental to the plant. BTS interaction with Fe, through its hemerythrin (HHE) domains, leads to its destabilisation. In this proposed model ILR3 and BTS play a central role in controlling the transcriptional machinery that regulates Fe homeostasis. Model adapted from Li *et al.* (2016).

repressor of glucosinolate biosynthesis, a class of secondary metabolites conferring resistance against several pathogens, confirming the dual role of ILR3 in regulating genes expression (Li *et al.*, 2014; Samira *et al.*, 2018).

The tight connection between ILR3 activity and ferritins accumulation, together with the strong similarity of *ilr3-1* and *fer1,3,4* (triple mutant deprived of ferritins in vegetative tissues) mutant responses to Fe availability (Figs S12, S13, S15), support that ILR3 integration of Fe signals to adjust plant development partly relies on ferritins. This hypothesis was confirmed by overexpressing *AtFER1* (*Pro35S:FER1*) in *ilr3-1* mutant (Figs 6, S14).

ILR3 and BTS are central to the regulation of Fe homeostasis

Recent studies have shown the upstream position of ILR3, bHLH34, bHLH104 and bHLH115 in the Fe deficiency transcriptional regulatory network (Li *et al.*, 2016; Liang *et al.*, 2017). However, the peculiar nature of ILR3 in regulating Fe homeostasis was not fully assessed, most probably because ILR3 displays redundant activities with bHLH34, bHLH104 and bHLH115. The only evidence reported so far was that *ilr3* loss-of-function mutants displayed the strongest Fe deficiency phenotype when compared with the other class IVc bHLH mutants

when grown in low Fe availability (Zhang *et al.*, 2015; Li *et al.*, 2016; Liang *et al.*, 2017). BTS (BRUTUS), a Fe binding E3 ubiquitin ligase, specifically targets ILR3, bHLH104 and bHLH115 leading to their degradation through the 26S proteasome (Selote *et al.*, 2015; Matthiadis & Long, 2016). BTS contains a hemerythrin-like domain able to bind Fe. The binding of Fe to the hemerythrin-like domain of BTS participates in its destabilisation and subsequent degradation (Selote *et al.*, 2015; Matthiadis & Long, 2016). Therefore, BTS was seen as the main regulator of Fe homeostasis, even if the link between BTS and the plant response to Fe excess was not clearly established.

The data presented in this study support that, unlike its closet homologues, ILR3 represses the expression of the main markers of the plant response to Fe excess, the ferritin genes (Figs 1, S4). In addition, our data indicate that ILR3 and PYE repress the expression of a common set of target genes (Figs 2–4, S6, S11), most probably through the formation of heterodimers (Fig. 5; Long *et al.*, 2010; Zhang *et al.*, 2015). Last, our data suggest that the regulation of *PYE* expression might rely on a negative feedback regulatory loop involving the ILR3-PYE complex. Altogether, these findings highlight the dual and unique role played by ILR3 in regulating the plant responses to fluctuations in Fe availability in the growth medium.

bHLH34, *bHLH104*, *bHLH115*, *ILR3* and *PYE* are mainly expressed in the pericycle cells (Long *et al.*, 2010; Rodríguez-Celma *et al.*, 2013b), which is the place of accumulation of ferritins in response to Fe excess in roots (Reyt *et al.*, 2015), and consistent with the repressive role of PYE on ferritin genes expression under Fe deficiency. Interestingly, the extent of the induction of *bHLH34*, *bHLH104*, *bHLH115* and *ILR3* transcript abundance in response to Fe deficiency is less pronounced than that of *PYE* (Zhang *et al.*, 2015; Liang *et al.*, 2017) (Figs 2d, S5, S11c). By contrast, Fe excess had no striking effect on *ILR3* or *PYE* mRNA abundance, compared with control condition (Figs 2d, S5, S11c). Therefore, assuming that the relative mRNA abundance of the bHLH IVc on the one hand and *PYE* on the other reflects the amount of ILR3-dependent protein complexes acting as activator (that is bHLH34-ILR3, bHLH104-ILR3 and bHLH115-ILR3) or repressor (that is PYE-ILR3), it can be hypothesised that the stoichiometry between the two types of complex would be modified by the Fe conditions (deficiency vs excess). In this model, the formation of the PYE-ILR3 complex is triggered in response to Fe deficiency by the ILR3-dependent activating protein complexes favouring the repression of ILR3 target genes. The recent work, which shows that ILR3 and PYE function in a regulatory network that controls wounding pathogen response, clearly reinforces this hypothesis (Samira *et al.*, 2018).

Taken together, the data gathered herein and in previous studies suggest that ILR3 and BTS play a central role in the machinery controlling Fe homeostasis (Fig. 8). In this model ILR3, whose activity is regulated by BTS in a Fe-dependent manner, acts as both a transcriptional activator of plant responses to Fe shortage and as a repressor of plant responses to Fe excess. Such regulatory loops between ILR3 and BTS, through the modulation of the equilibrium between the different ILR3-dependent protein complexes, most probably ensure the dynamic and balanced expression of genes involved in Fe homeostasis in accordance with Fe availability.

Acknowledgements

ilr3-1 seeds were kindly provided by Prof. Bonnie Bartel (Rice University, Houston, Texas, USA). The *ProPYE:gPYE:GFP* line was kindly provided by Prof. Terry A Long (North Carolina State University, Raleigh, North Carolina, USA). We thank Dr Carine Alcon and the Montpellier Rio-Imaging platform (Plateforme PHIV La Gaillarde) for expertise and assistance in microscopy and Sandrine Chay (BPMP, SAME platform) for technical support in plant Fe determination. NT and FB were supported by a fellowship from the French 'Ministère de l'Enseignement Supérieur et de la Recherche'. KR and FG were supported by a fellowship from the Agence Nationale pour la Recherche (ANR-17-CE20-0008-01) and from the China Scholarship Council (CSC), respectively. SG-G's work was supported by CONICYT-Chile grant 21170951. HR was funded by FONDECYT 1160334 (Chilean Government) grant. This work was also supported by the CONICYT-ECOS project C18B04. We thank Dr N. Berger for help in preparing this manuscript.

Author contributions

Conceived and designed the experiments: NT, KR, FGao, SGG, FB, EI, AMartin, FV, HR, CD. Performed the experiments: NT, KR, SGG, FGao, JB, FB, AMaghiaoui, RM, EI, MB, FV, CD. Analysed the data: NT, KR, SGG, FGao, FB, EI, MB, AMartin, FV, HR, FGaymard, JFB, CD. Contributed reagents/materials/analysis tools: NT, KR, FGao, FB, EI, MB, AMartin, FV, HR, FGaymard, CD. Wrote the paper: NT, FGaymard, JFB, CD. KR and FGao contributed equally to this work.

ORCID

Fanny Bellegarde https://orcid.org/0000-0001-7221-5033
Christian Dubos https://orcid.org/0000-0001-5486-3643
Fei Gao https://orcid.org/0000-0002-4347-8499
Esther Izquierdo https://orcid.org/0000-0003-0448-4447
Antoine Martin https://orcid.org/0000-0002-6956-2904
Hannetz Roschzttardtz https://orcid.org/0000-0002-2614-2504
Florence Vignols https://orcid.org/0000-0002-2031-0407

References

Aparicio F, Pallas V. 2016. The coat protein of *Alfalfa mosaic* virus interacts and interferes with the transcriptional activity of the bHLH transcription factor ILR3 promoting salicylic-dependent defense signaling response. *Molecular Plant Pathology* **18**: 173–186.

Becker A. 2005. Iron toxicity in rice: conditions and management concepts. *Journal of Plant Nutrition and Soil Science* **168**: 558–573.

Bournier M, Tissot N, Mari S, Boucherez J, Lacombe E, Briat JF, Gaymard F. 2013. Arabidopsis ferritin 1 (AtFer1) gene regulation by the phosphate

starvation response 1 (AtPHR1) transcription factor reveals a direct molecular link between iron and phosphate homeostasis. *Journal of Biological Chemistry* **288**: 22670–22680.

Briat JF, Dubos C, Gaymard F. 2015. Iron nutrition, biomass production, and plant product quality. *Trends in Plant Science* **20**: 33–40.

Briat JF, Duc C, Ravet K, Gaymard F. 2010. Ferritins and iron storage in plants. *Biochimica et Biophysica Acta* **1800**: 806–814.

Brumbarova T, Bauer P, Ivanov R. 2015. Molecular mechanisms governing Arabidopsis iron uptake. *Trends in Plant Science* **20**: 124–133.

Colangelo EP, Guerinot ML. 2004. The essential basic helix-loop-helix protein FIT1 is required for the iron deficiency response. *Plant Cell* **16**: 3400–3412.

Connorton JM, Balk J, Rodríguez-Celma J. 2017. Iron homeostasis in plants – a brief overview. *Metallomics* **9**: 813–823.

Cui Y, Chen CL, Cui M, Zhou WJ, Wu HL, Ling HQ. 2018. Four IVa bHLH transcription factors are novel interactors of FIT and mediate JA inhibition of iron uptake in Arabidopsis. *Molecular Plant* **11**: 1166–1183.

Curie C, Mari S. 2016. New routes for plant iron mining. *New Phytologist* **214**: 521–525.

De Masi F, Grove CA, Vedenko A, Alibes A, Gisselbrecht SS, Serrano L, Bulyk ML, Walhout AJ. 2011. Using a structural and logics systems approach to infer bHLH-DNA binding specificity determinants. *Nucleic Acids Research* **39**: 4553–4563.

Duc C, Cellier F, Lobreaux S, Briat JF, Gaymard F. 2009. Regulation of iron homeostasis in *Arabidopsis thaliana* by the clock regulator time for coffee. *Journal of Biological Chemistry* **284**: 36271–36281.

Eide D, Broderius M, Fett J, Guerinot ML. 1996. A novel iron-regulated metal transporter from plants identified by functional expression in yeast. *Proceedings of the National Academy of Sciences, USA* **93**: 5624–5628.

Fourcroy P, Siso-Terraza P, Sudre D, Saviron M, Reyt G, Gaymard F, Abadia A, Abadia J, Alvarez-Fernandez A, Briat JF. 2014. Involvement of the ABCG37 transporter in secretion of scopoletin and derivatives by Arabidopsis roots in response to iron deficiency. *New Phytologist* **201**: 155–167.

Fourcroy P, Tissot N, Gaymard F, Briat JF, Dubos C. 2016. Facilitated Fe nutrition by phenolic compounds excreted by the Arabidopsis ABCG37/PDR9 transporter requires the IRT1/FRO2 high-affinity root Fe^{2+} transport system. *Molecular Plant* **9**: 485–488.

Fourcroy P, Vansuyt G, Kushnir S, Inze D, Briat JF. 2004. Iron-regulated expression of a cytosolic ascorbate peroxidase encoded by the *APX1* gene in Arabidopsis seedlings. *Plant Physiology* **134**: 605–613.

Gao F, Robe K, Gaymard F, Izquierdo E, Dubos C. 2019. The transcriptional control of iron homeostasis in plants: a tale of bHLH transcription factors? *Frontiers in Plant Science* **10**: 006.

Gollhofer J, Schlawicke C, Jungnick N, Schmidt W, Buckhout TJ. 2011. Members of a small family of nodulin-like genes are regulated under iron deficiency in roots of *Arabidopsis thaliana*. *Plant Physiology and Biochemistry* **49**: 557–564.

Gollhofer J, Timofeev R, Lan P, Schmidt W, Buckhout TJ. 2014. Vacuolar-Iron-Transporter1-Like proteins mediate iron homeostasis in Arabidopsis. *PLoS ONE* **9**: e110468.

Guerinot ML, Yi Y. 1994. Iron: nutritious, noxious, and not readily available. *Plant Physiology* **104**: 815–820.

Heim MA, Jakoby M, Werber M, Martin C, Weisshaar B, Bailey PC. 2003. The basic helix-loop-helix transcription factor family in plants: a genome-wide study of protein structure and functional diversity. *Molecular Biology and Evolution* **20**: 735–747.

Henriques R, Jasik J, Klein M, Martinoia E, Feller U, Schell J, Pais MS, Koncz C. 2002. Knock-out of Arabidopsis metal transporter gene *IRT1* results in iron deficiency accompanied by cell differentiation defects. *Plant Molecular Biology* **50**: 587–597.

Hentze MW, Muckenthaler MU, Galy B, Camaschella C. 2010. Two to tango: regulation of Mammalian iron metabolism. *Cell* **142**: 24–38.

Jakoby M, Wang HY, Reidt W, Weisshaar B, Bauer P. 2004. FRU (BHLH029) is required for induction of iron mobilization genes in *Arabidopsis thaliana*. *FEBS Letters* **577**: 528–534.

Kagale S, Rozwadowski K. 2011. EAR motif-mediated transcriptional repression in plants: an underlying mechanism for epigenetic regulation of gene expression. *Epigenetics* **6**: 141–146.

Khabaz-Saberi R. 2010. Aluminium, manganese, and ion tolerance improves performance of wheat genotypes in waterlogged acidic soils. *Journal of Plant Nutrition and Soil Science* **173**: 461–468.

Klatte M, Schuler M, Wirtz M, Fink-Straube C, Hell R, Bauer P. 2009. The analysis of Arabidopsis nicotianamine synthase mutants reveals functions for nicotianamine in seed iron loading and iron deficiency responses. *Plant Physiology* **150**: 257–271.

Kobayashi T, Nishizawa NK. 2012. Iron uptake, translocation, and regulation in higher plants. *Annual Review of Plant Biology* **63**: 131–152.

Li B, Gaudinier A, Tang M, Taylor-Teeples M, Nham NT, Ghaffari C, Benson DS, Steinmann M, Gray JA, Brady SM *et al.* 2014. Promoter-based integration in plant defense regulation. *Plant Physiology* **166**: 1803–1820.

Li X, Zhang H, Ai Q, Liang G, Yu D. 2016. Two bHLH transcription factors, bHLH34 and bHLH104, regulate iron homeostasis in *Arabidopsis thaliana*. *Plant Physiology* **170**: 2478–2493.

Liang G, Zhang H, Li X, Ai Q, Yu D. 2017. bHLH transcription factor bHLH115 regulates iron homeostasis in *Arabidopsis thaliana*. *Journal of Experimental Botany* **68**: 1743–1755.

Long TA, Tsukagoshi H, Busch W, Lahner B, Salt DE, Benfey PN. 2010. The bHLH transcription factor POPEYE regulates response to iron deficiency in Arabidopsis roots. *Plant Cell* **22**: 2219–2236.

Matthiadis A, Long TA. 2016. Further insight into BRUTUS domain composition and functionality. *Plant Signal & Behavior* **11**: e1204508.

Meinke DW. 2013. A survey of dominant mutations in *Arabidopsis thaliana*. *Trends in Plant Science* **18**: 84–91.

Morrissey J, Guerinot ML. 2009. Iron uptake and transport in plants: the good, the bad, and the ionome. *Chemical Reviews* **109**: 4553–4567.

Nechushtai R, Conlan AR, Harir Y, Song L, Yogev O, Eisenberg-Domovich Y, Livnah O, Michaeli D, Rosen R, Ma V *et al.* 2012. Characterization of Arabidopsis NEET reveals an ancient role for NEET proteins in iron metabolism. *Plant Cell* **24**: 2139–2154.

Palmer CM, Hindt MN, Schmidt H, Clemens S, Guerinot ML. 2013. MYB10 and MYB72 are required for growth under iron-limiting conditions. *PLoS Genet* **9**: e1003953.

Paz-Ares J. 2002. REGIA, an EU project on functional genomics of transcription factors from *Arabidopsis thaliana*. *Comparative and Functional Genomics* **3**: 102–108.

Petit JM, van Wuytswinkel O, Briat JF, Lobreaux S. 2001. Characterization of an iron-dependent regulatory sequence involved in the transcriptional control of *AtFer1* and *ZmFer1* plant ferritin genes by iron. *Journal of Biological Chemistry* **276**: 5584–5590.

Rampey RA, Woodward AW, Hobbs BN, Tierney MP, Lahner B, Salt DE, Bartel B. 2006. An Arabidopsis basic helix-loop-helix leucine zipper protein modulates metal homeostasis and auxin conjugate responsiveness. *Genetics* **174**: 1841–1857.

Ravet K, Touraine B, Boucherez J, Briat JF, Gaymard F, Cellier F. 2009. Ferritins control interaction between iron homeostasis and oxidative stress in Arabidopsis. *The Plant Journal* **57**: 400–412.

Reyt G, Boudouf S, Boucherez J, Gaymard F, Briat JF. 2015. Iron- and ferritin-dependent reactive oxygen species distribution: impact on Arabidopsis root system architecture. *Molecular Plant* **8**: 439–453.

Robinson NJ, Procter CM, Connolly EL, Guerinot ML. 1999. A ferric-chelate reductase for iron uptake from soils. *Nature* **397**: 694–697.

Rodríguez-Celma J, Lin WD, Fu GM, Abadia J, Lopez-Millan AF, Schmidt W. 2013a. Mutually exclusive alterations in secondary metabolism are critical for the uptake of insoluble iron compounds by Arabidopsis and *Medicago truncatula*. *Plant Physiology* **162**: 1473–1485.

Rodríguez-Celma J, Pan IC, Li W, Lan P, Buckhout TJ, Schmidt W. 2013b. The transcriptional response of Arabidopsis leaves to Fe deficiency. *Frontiers in Plant Science* **4**: 276.

Roschzttardtz H, Conejero G, Curie C, Mari S. 2009. Identification of the endodermal vacuole as the iron storage compartment in the Arabidopsis embryo. *Plant Physiology* **151**: 1329–1338.

Roschzttardtz H, Conejero G, Divol F, Alcon C, Verdeil JL, Curie C, Mari S. 2013. New insights into Fe localization in plant tissues. *Frontiers in Plant Science* **4**: 350.

Samira R, Li B, Kliebenstein D, Li C, Davis E, Gillikin JW, Long TA. 2018. The bHLH transcription factor ILR3 modulates multiple stress responses in Arabidopsis. *Plant Molecular Biology* **97**: 297–309.

Santi S, Schmidt W. 2009. Dissecting iron deficiency-induced proton extrusion in Arabidopsis roots. *New Phytologist* **183**: 1072–1084.

Schmid NB, Giehl RF, Doll S, Mock HP, Strehmel N, Scheel D, Kong X, Hider RC, von Wiren N. 2014. Feruloyl-CoA 6′-Hydroxylase1-dependent coumarins mediate iron acquisition from alkaline substrates in Arabidopsis. *Plant Physiology* **164**: 160–172.

Selote D, Samira R, Matthiadis A, Gillikin JW, Long TA. 2015. Iron-binding E3 ligase mediates iron response in plants by targeting basic helix-loop-helix transcription factors. *Plant Physiology* **167**: 273–286.

Strozycki PM, Szymanski M, Szczurek A, Barciszewski J, Figlerowicz M. 2010. A new family of ferritin genes from *Lupinus luteus* – comparative analysis of plant ferritins, their gene structure, and evolution. *Molecular Biology and Evolution* **27**: 91–101.

Varotto C, Maiwald D, Pesaresi P, Jahns P, Salamini F, Leister D. 2002. The metal ion transporter IRT1 is necessary for iron homeostasis and efficient photosynthesis in *Arabidopsis thaliana*. *The Plant Journal* **31**: 589–599.

Vert G, Grotz N, Dedaldechamp F, Gaymard F, Guerinot ML, Briat JF, Curie C. 2002. IRT1, an Arabidopsis transporter essential for iron uptake from the soil and for plant growth. *Plant Cell* **14**: 1223–1233.

Wang HY, Klatte M, Jakoby M, Baumlein H, Weisshaar B, Bauer P. 2007. Iron deficiency-mediated stress regulation of four subgroup Ib BHLH genes in *Arabidopsis thaliana*. *Planta* **226**: 897–908.

Wang N, Cui Y, Liu Y, Fan H, Du J, Huang Z, Yuan Y, Wu H, Ling HQ. 2013. Requirement and functional redundancy of Ib subgroup bHLH proteins for iron deficiency responses and uptake in *Arabidopsis thaliana*. *Molecular Plant* **6**: 503–513.

Yuan Y, Wu H, Wang N, Li J, Zhao W, Du J, Wang D, Ling HQ. 2008. FIT interacts with AtbHLH38 and AtbHLH39 in regulating iron uptake gene expression for iron homeostasis in Arabidopsis. *Cell Research* **18**: 385–397.

Zhang J, Liu B, Li M, Feng D, Jin H, Wang P, Liu J, Xiong F, Wang J, Wang HB. 2015. The bHLH transcription factor bHLH104 interacts with IAA-LEUCINE RESISTANT3 and modulates iron homeostasis in Arabidopsis. *Plant Cell* **27**: 787–805.

Supporting Information

Additional Supporting Information may be found online in the Supporting Information section at the end of the article.

Fig. S1 Histochemical detection of GUS activity in 2-wk-old seedlings driven by *ProAtFER1* 5′-end deletion and site-directed mutagenesis constructs.

Fig. S2 Schematic representation of conserved DNA regions (elements) and *cis*-regulatory sequences present in the 500 bp upstream from the transcription initiation sequence of the three main ferritin genes expressed in vegetative tissues.

Fig. S3 Genome Browser snapshots of ATAC-seq, and H3K9ac, H3K4me3 and H3K27me3 ChIP-seq peaks on the three main ferritin genes found in *Arabidopsis thaliana* vegetative tissues, namely *AtFER1*, *AtFER3* and *AtFER4*.

Fig. S4 Yeast one-hybrid (Y1H) screen using *ProAtFER1* Element 5 as bait.

Fig. S5 *ilr3-3* and *ilr3-1* express a loss-of-function and a dominant mutant allele of *ILR3*, respectively.

Fig. S6 ILR3 is a repressor of ferritin genes expression.

Fig. S7 ILR3 repression of ferritins expression is unique within the clade IVc bHLHs TFs implicated in the transcriptional control of iron deficiency responses.

Fig. S8 ILR3 acts as both transcriptional activator and repressor to regulate Fe homeostasis.

Fig. S9 *ilr3-3* complementation experiment using *ProILR3:ILR3:GFP*.

Fig. S10 Genome Browser snapshots of ATAC-seq, and H3K9ac, H3K4me3 and H3K27me3 ChIP-seq peaks on the *Arabidopsis thaliana NICOTIANAMINE SYNTHASE 4* gene (*NAS4*).

Fig. S11 ILR3 and PYE regulate common set of genes.

Fig. S12 Fe-dependent seedling root growth involves ILR3 and ferritins activity.

Fig. S13 Fe-dependent seedling fresh weight involves ILR3 and ferritins activity.

Fig. S14 Complementation of *ilr3-1* seedling fresh weight phenotype by overexpressing *AtFER1*

Fig. S15 ILR3 participates to the plant response to Fe excess.

Fig. S16 Overexpression of *AtFER1* rescue *ilr3-1* sensitivity to Fe excess.

Fig. S17 ILR3 modulates Fe content.

Methods S1 Detailed protocols used in this study for physiological, biochemical, molecular and cytological analyses.

Table S1 Primers used in this study.

Please note: Wiley Blackwell are not responsible for the content or functionality of any Supporting Information supplied by the authors. Any queries (other than missing material) should be directed to the *New Phytologist* Central Office.

See also the Commentary on this article by Kroh & Pilon, **223**: 1052–1055.